International Journal of Chemical Studies

P-ISSN: 2349-8528
E-ISSN: 2321-4902
www.chemijournal.com
IJCS 2025; 13(3): 11-20

Received: 12-02-2025
Accepted: 18-03-2025

Irina Korotkova
Department of Biotechnology and Chemistry, Poltava State Agrarian University, Skovorody, Poltava, Ukraine

Tamila Romashko
Department of Biotechnology and Chemistry, Poltava State Agrarian University, Skovorody, Poltava, Ukraine

Oleg Khakhel
Department of Biotechnology and Chemistry, Poltava State Agrarian University, Skovorody, Poltava, Ukraine

Corresponding Author:
Irina Korotkova
Department of Biotechnology and Chemistry, Poltava State Agrarian University, Skovorody, Poltava, Ukraine

Synchronous fluorescence spectroscopy for investigating aggregation phenomena in polymer matrix

Irina Korotkova, Tamila Romashko and Oleg Khakhel

DOI: https://www.doi.org/10.22271/chemi.2025.v13.i3a.12533

Abstract
Organic photoluminescent materials, such as fluorescent polymers and small fluorescent molecules, are widely used in optoelectronics, sensing, bioimaging, and related fields. However, their practical application is often limited by aggregation-induced fluorescence quenching in concentrated solutions or solid-state environments. To enable rational use of such materials, spectroscopic tools capable of detecting spectral manifestations of aggregation are essential. In this study, we proposed the use of synchronous fluorescence spectroscopy (SFS) to investigate aggregation-related spectral features in various polymer matrices containing phenyl-based chromophores and some aromatic compounds, including 9,10-diphenylanthracene, pyrene, anthracene, and naphthalene. SFS exhibited high sensitivity in identifying aggregate-related spectral features, including excimer-like emission and bathochromic shifts, both in solid matrices and liquid media. The results demonstrate that SFS is an effective diagnostic tool for probing aggregation behavior and optimizing the photophysical properties of polymeric luminescent materials.

Keywords: Spectral manifestations of aggregation, dimer, excimer, synchronous fluorescence spectroscopy

Introduction
Over the past decades, intensive experimental and theoretical studies have led to the widespread use of organic photoluminescent materials, particularly aromatic fluorescent molecules, in diverse applications such as sensing (Weldeab *et al.*, 2018) [1] and imaging (Saremi *et al.*, 2020) [2], Yamagishi *et al.*, 2021) [3], optoelectronics (Li *et al.*, 2015) [4], fluorescent bioprobes (Liu *et al.*, 2018) [5], molecular imaging (Lichon *et al.*, 2020) [6], (Korneev *et al.*, 2019) [7], OLED (Li *et al.*, 2019) [8], etc. The traditional organic photoluminescent materials contain predominantly π-π-conjugated structures. And although they have use for many years, some moments greatly impeded their practical applications in optoelectronic devices and biological applications, including a strong tendency to aggregate in concentrated solutions and the solid state, leading to fluorescence quenching (Jiang *et al.*, 2021) [9].
Luminescent molecular systems for most optoelectronic applications are used as thin polymer films (Bu *et al.*, 2023) [10], (De *et al.*, 2017) [11], whereas for chemical and biological applications they are used in solutions and physiological environments where they exhibit high emission. In the solid state, due to strong π-π stacking interactions that promote excimer formation, the emission of such systems is significantly quenched.
Currently, two major branches for creation of such materials are distinguished: polymers chain with fluorophores in their structure and polymers with phenomena of aggregation-induced emission. In the first case, the conjugated polymer contains a fluorophore imparting photoluminescent properties to the final material, offering tunable structures, robust mechanical properties and other unique properties, but these materials cannot avoid the aggregation-caused quenching (ACQ) problem (Huang *et al.*, 2019) [12]. In the second case, polymers exhibit high fluorescence efficiency in the solid state due to the fluorescent aggregates formation-aggregation-induced emission (AIE). The main technique for AIE polymers designing is the integration of aggregation-induced emission materials into polymer

structures or attaching emitting polymer pendants by polymerization and modification (Ahumada *et al.*, 2022) [13]. The advantage of polymers containing fluorophores is their intense photoluminescence, which determines their wide application, including in optoelectronic devices. But the nature of the polymers causes a stable tendency of fluorophores to aggregate, leading to strong quenching of fluorescence, which significantly limits their practical application. The formation of aggregates leads to broad and featureless bands appearing in fluorescence spectra (Fakis *et al.*, 2006) [14].

Fluorescence spectra of condensed systems containing aromatic chromophores are characterized by variations in the manifestations of different forms of aggregates (Yuzhakov, 1992) [15], (Ma *et al.*, 2021) [16], (Heo *et al.*, 2022) [17]. However, the identification of bands in the fluorescence spectra of such systems, as well as the determination of the nature of the electronic states, presents significant challenges. Among the associated forms of such systems are molecular excimers, whose spectral bands are difficult to distinguish.

Excimers are dimers formed by two identical atoms or molecules, which unstable in the ground state and formed only at excitation system. Planar aromatic molecules are easy to form excimer in the concentrated solution or solid state, because of the intermolecular π-π interactions. After pyrene, the first aromatic molecule exhibits excimer fluorescence in solution, other aromatic systems (benzene, naphthalene, anthracene, etc.) have been also recorded, forming excimer structures in rigid media of solid polymer systems (polymer films), in crystals, supramolecular systems, etc (Schillmöller *et al.*, 2021) [18], (Gao *et al.*, 2018) [19]. In a crystal, such systems usually tend to form infinite herringbone arrangement, despite this is far from only a single and pure excimer formation. The most desirable aggregation mode in crystal is an isolated aromatic dimer with the perfectly cofacial π-π stacking.

Spectral manifestation of excimers formation is an emission band with an anomalously large Stokes shift to longer wavelengths. This phenomenon is not accompanied by qualitative changes in the absorption spectra of the studied systems. The absorption spectra of the molecules forms the excimers are similar to the monomer molecule absorption spectra, indicating the absence of aggregation in the ground state (Zhao *et al.*, 2022) [20].

Excimer emission is characterized by a bathochromic shift of the fluorescence spectra resulting from the interaction between molecules in close contact. The shift magnitude depends on the molecular interactions and molecular packing structure (Lee *et al.*, 2016) [21]. The excimer formation and their fluorescence can be modulated by the concentration of the corresponding monomers and external factors such as pH, environmental temperature, solvent polarity and intermolecular interactions (Hoche *et al.*, 2017) [22], (Li *et al.*, 2014) [23]. This allows the use of the molecular systems with excimer emission for a various applications (Chen, 2022) [24], (Dai *et al.*, 2024) [25], (Casier & Duhamel, 2022) [26].

Although many experimental and theoretical studies have focused on the relationship between the aggregate structure and emission properties of a wide range of chromophore-containing polymeric materials, a better understanding of the spectral manifestations of excimer formation remains a key topic for the targeted rational design of organic π-conjugated materials with desired optoelectronic properties.

Considering the significant number of experimental and theoretical studies on the relationship between aggregate structure and the emission properties of a wide range of chromophore-containing polymeric materials, there is a need to consolidate existing data for the targeted and rational design of organic π-conjugated materials with desired optoelectronic properties. An important step in this process is the application of methods for reliable identification of spectral bands in the fluorescence spectra of such systems. A simple and elegant method to differentiating the fluorescence spectra of compounds in solution − synchronous fluorescence spectroscopy − was first proposed by Lloyd (1971) [27] and later developed for solid samples, including polymers and their complexes with chromophore molecules, inorganic compounds, and coordination complexes by Vo-Dinh (1978) [28], Cabaniss (1991) [29], and others (Tian *et al.*, 2025) [30]. Considering its numerous advantages, this method has been employed in the present work.

The aim of this study is to investigate the spectral manifestations of aggregation in polymer systems containing phenyl chromophores, as well as polymers containing 9,10-diphenylanthracene, pyrene, anthracene, and naphthalene, using synchronous fluorescence spectroscopy.

Materials and Methods

A series of model systems were prepared for spectral measurements, as follows:

1. An aqueous solution of a copolymer of polyvinyl alcohol (PVA) with 9-anthraldehyde (1.5g L^{-1}) with a molar ratio of PVA and fluorophore of 4.3 : 100 (Fig. 1);
2. A solid solution of anthracene in polymethyl methacrylate (PMMA) at concentrations of 0.5% and 2% (Fig. 2);
3. A solid solution of 9-vinylanthracene in PolyDiethyleneglycol-bisallyl carbonate (PDEAC) (Fig. 3);
4. A copolymer of 9,10-dibenzanthracene with PVA (Fig. 4);
5. A pyrene solution in chloroform and water (saturated and diluted 1000-fold), (Fig. 5, 6);
6. A composition of cycloaliphatic epoxy resin (UP-612) with 20% naphthalene (Fig. 7);
7. A copolymer of methyl methacrylate (MMA) with naphthyl methacrylate in concentrations of 0.1 and 0.5 mol% (Fig. 8);
8. Benzene solution;
9. Polystyrene films.

Polymer films based on PVA

Polymer films were prepared by treating a PVA solution with the low-molecular-weight luminophore 9,10-dibenzanthracene at a molar ratio of PVA to luminophore of 1000:1 in an N,N-dimethylacetamide (DMA) medium. *p*-Toluenesulfonic acid (5% by weight of PVA) was added as a catalyst, and the reaction was conducted at a temperature range of 100-140 °C. The resulting polymer solution was poured into excess acetone. After stirring in acetone for 1 hour, the polymer precipitate was filtered and air-dried for 6 hours. The dried polymer was then redissolved in hot water and purified by reprecipitation, repeating this process three times with excess acetone. The purified polymer was dried in a vacuum at 50 °C to a constant weight. The resulting polymer films were used for subsequent spectral measurements.

Polymer samples based on PMMA

The solid solutions of anthracene in PMMA at concentrations of 0.5% and 2% were prepared using a two-stage bulk

polymerization method. In the first stage, polymerization was carried out at 50c for 24 hours, followed by post-polymerization at 115 °C for 6 hours. Azoisobutyronitrile was used as the initiator at a concentration of 0.06 mol%. The polymerization process was carried out under an inert atmosphere (nitrogen) to prevent oxidation. After polymerization, the resulting solid polymer was purified by washing with acetone to remove unreacted monomers and anthracene. The purified solid solution was dried in a vacuum at 50 °C to a constant weight.

Polymer samples based on MMA with naphthyl methacrylate

To obtain a copolymer of methyl methacrylate (MMA) with naphthyl methacrylate at concentrations of 0.1 and 0.5 mol%, the MMA monomer was first purified by distillation and filtration through membrane filters to remove impurities. Naphthyl methacrylate was then mixed with the purified MMA in the indicated desired molar ratios. The polymerization mixtures were degassed by subjecting them to several freeze-thaw cycles to remove oxygen and prevent premature polymerization. The degassed mixtures were then placed in glass molds under a vacuum to ensure uniformity. Polymerization was carried out at a controlled temperature, and after completion, the samples (1 mm thick plates) were removed from the molds. The resulting copolymers were washed with an acetone to remove unreacted monomers and were then dried in a vacuum at 50 °C until a constant weight was reached.

Polymer samples of cycloaliphatic epoxy resin with 20% naphthalene

A composition of cycloaliphatic epoxy resin (UP-612) with 20% naphthalene was prepared by dissolving 20 g of naphthalene in the resin under heated to 50-60 °C. The naphthalene was completely dissolved under stirring until a homogeneous solution was obtained. To ensure a uniform dispersion, the mixture was stirred for an additional 30 minutes at the same temperature. Afterward, the composition was cooled to room temperature and degassed under vacuum to remove any air bubbles that may have formed during the mixing process.

Solid samples of 9-vinylanthracene in PDEAC

A solid solution of 9-vinylanthracene in poly(diethyleneglycol bisallyl carbonate) (PDEAC) was prepared via thermal bulk polymerization under a stepwise temperature increase in the range of 85-120 °C. Prior to polymerization, 9-vinylanthracene was added to diethyleneglycol bisallyl carbonate at a concentration of 1% and stirred at room temperature until a homogeneous solution was obtained. The mixture was then poured into glass molds. Polymerization was initiated at 85 °C for 6 hours and continued with gradual heating to 120 °C over the next 12 hours. Diisopropyl peroxydicarbonate was used as the initiator at a concentration of 0.1%. After polymerization, the solid samples were cooled to room temperature, removed from the molds, and used without further purification for spectral measurements.

Polystyrene films

Polystyrene films were prepared by dissolving polystyrene in chloroform to obtain a 5% solution. The solution was cast onto clean glass substrates and allowed to dry at room temperature under ambient conditions. After solvent evaporation, the films were additionally dried in a vacuum oven at 40 °C for 12 hours to ensure complete removal of residual solvent. The resulting transparent films were peeled off and used for fluorescence spectral measurements.

Spectral measurements

Fluorescence and synchronous fluorescence spectra of the studied samples were recorded using a PerkinElmer LS-45 fluorescence spectrometer. Both the excitation and emission bandwidths were set to 5 nm. The spectral range was 200-700 nm. The measurement error for band positions was±2 nm, and the spectral band half-width was 5 nm. Synchronous fluorescence spectra were recorded at a scanning rate of 240 nm/min with various monochromator offset values ($\Delta\lambda$) ranging from 0 to 30 nm, as determined by the intensity of scattered light from the excitation source by the object of study.

Thin quartz cuvettes of the "spatula" type were used for measuring the fluorescence intensity of liquid solutions. The excitation of fluorescence was performed under frontal illumination of the cuvette, with the incident light directed perpendicularly to the sample surface.

As is well known, the fluorescence intensity of concentrated solutions and solid samples is significantly reduced due to the inner filter effect. Therefore, during the recording of synchronous fluorescence spectra, the excitation light beam was directed onto the sample cuvette at an angle between 30° and 60° relative to its front surface. The use of this geometry is a standard practice in solid-state synchronous spectrofluorimetry (Samokhvalov, 2020) [31]. In our studies, the planes of both the cuvette and the polymer films were oriented at an angle of approximately 30° between them and the direction of the excitation light beam.

To suppress scattered light from the excitation source, during the recording of synchronous fluorescence spectra in the "without wavelength offsets between the excitation and emission monochromators" mode, film polarizers with a working range of 200-750 nm, supplied with the spectrometer, were used.

Solid solution samples were placed in the cuvette compartment using a special holder. The orientation of the samples was adjusted to be optimal for recording fluorescence via reflection with minimal losses due to reabsorption of emission.

Results and Discussion

Aggregation of chromophores, which commonly occurs in highly concentrated solutions or in the solid state, typically leads to fluorescence quenching – a phenomenon known as aggregation-caused quenching (ACQ). This effect complicates the study of absorption spectra, as measurements must be conducted outside the monomer absorption band to avoid distortions. In contrast, fluorescence-based techniques are widely regarded as the most effective tools for investigating the spectral manifestations of aggregation in aromatic chromophores.

To assess the aggregation behavior of aromatic chromophores in various environments, we conducted a series of fluorescence and synchronous fluorescence spectroscopy measurements on the prepared systems. The key findings are presented below.

In fluorescence spectroscopy, an emission spectrum is obtained by scanning the emission wavelength (λ_{em}) while keeping the excitation wavelength (λ_{exc}) fixed. However, this conventional method often produces unsatisfactory results due to poor spectral resolution. The resulting emission spectra

typically consist of broad, overlapping bands (often exceeding 50 nm in width), which complicates the identification of individual fluorescent species, including aggregates (Silveira & Barbeira, 2022) [32]. To overcome these limitations, the present study employed synchronous fluorescence spectroscopy (SFS) to investigate the spectral manifestations of aggregation. This technique enables the differentiation of spectral contributions from different components in the system (e.g., monomers and aggregates) by simultaneously scanning both the excitation and emission wavelengths (Samokhvalov, 2020) [31].

Depending on the scanning speeds of the radiation and the excitation of the monochromators (λ_{em} and λ_{exc}) and the type of maintained difference between them ($\Delta\lambda$), several methods of synchronous fluorescence have been developed. These methods are used both for spectroscopic studies and for determining certain thermodynamic parameters and the kinetics of polymer crystallization, which are associated with the evolution of macromolecular structure during the melting and crystallization process (Luo *et al.*, 2014) [33]. In this study, depending on the sample, synchronous fluorescence spectra were recorded with various monochromator offset values ($\Delta\lambda$) ranging from 0 to 30 nm.

Fluorescence and SFS Spectra of Model Systems

Figure 1 shows the effect of the wavelength offset between the excitation and emission monochromators on the appearance of the SFS spectra of an aqueous solution (1.5 g L^{-1}) of a PVA copolymer with 9-anthraldehyde, at a molar ratio of PVA to luminophore of 4.3 : 100.

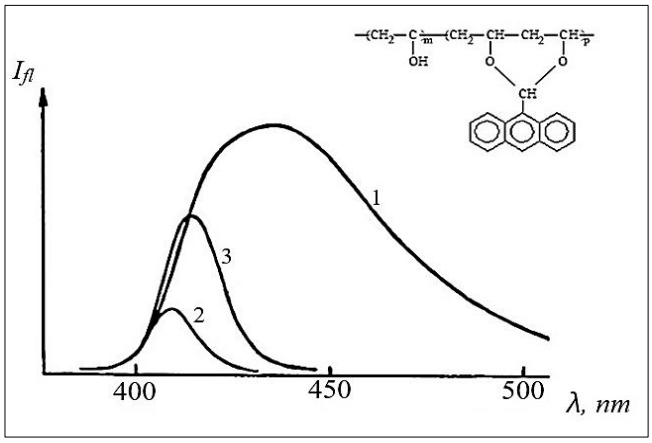

Fig 1: Fluorescence spectra of an aqueous solution of a copolymer of PVA with 9-anthraldehyde recorded at excitation wavelength λ_{exc} = 360 nm (curves 1) and SFS (curves 2 and 3) at $\lambda_{reg} = \lambda_{exc}$ (2) and $\lambda_{reg} = \lambda_{exc}+10$ nm (3). Wavelengths are indicated according to the registration scale.

The type of bond between the anthracene moiety and the main chain in this copolymer does not facilitate the formation of complexes between adjacent chromophores along the polymer backbone. As a result, its fluorescence in aqueous solution exhibits a monomeric character (Fig. 1, curve 1). The synchronous fluorescence (SFS) spectrum of the copolymer solution, recorded without any wavelength offset ($\Delta\lambda$ = 0 nm), also displays a single band with a maximum at approximately λ_{max} = 410 nm (Fig. 1, curve 2). When recorded with a wavelength offset of $\Delta\lambda$ = 10 nm, the SFS spectrum of the same solution (Fig. 1, curve 3) appears slightly broadened, and its maximum undergoes a bathochromic shift of about 4 nm compared to the $\Delta\lambda$ = 0 nm spectrum. Nevertheless, no distinct structural features are observed in this spectrum.

In solid films of this copolymer, the extended π-system of the anthracene moieties promotes strong polymer aggregation, leading to the appearance of an aggregate band in the SFS spectra within the 450-500 nm range. The fluorescence of these aggregates closely resembles that of anthracene aggregates embedded in PMMA (Fig. 2, curve 2). The pronounced red shift observed in the fluorescence spectra in the solid state may also be attributed to excimer formation (Congrave *et al.*, 2021) [34].

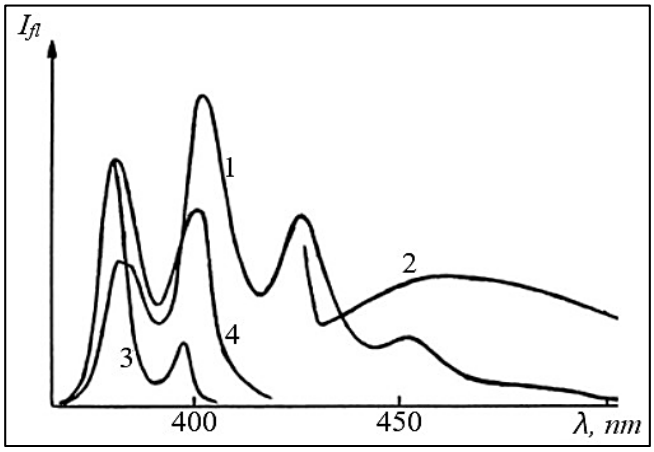

Fig 2: Fluorescence spectra of a solid solution of anthracene in PMMA (2%) at excitation λ_{exc} = 360 (1) and λ_{exc} = 420 (2) nm and SFS spectra of a solid solution of anthracene 0.5% (3) and 2% (4) in PMMA. Wavelengths are indicated according to the registration scale.

Figure 2 shows the fluorescence spectra of a solid solution (2%) of anthracene in PMMA at different excitation wavelengths: λ_{exc} = 360 nm (1) and λ_{exc} = 420 nm (2). We suggest that the intense maximum around ~400 nm (curve 1) should be associated with the fluorescence of the monomer, while the broad band in the bathochromic region around ~450-500 nm (curve 2) may be attributed to the fluorescence of the excimer.

However, in the SFS spectra of the anthracene solid solutions, the aggregate band appears only around ~430 nm. It should be noted that in the concentration range of 0.5-2%, the SFS spectra exhibit an intense band with a maximum at ~λ_{max} = 400 nm (Fig. 2, curves 3 and 4), indicating the formation of one type of aggregates. A comparison of spectra 3 and 4 in Fig. 2, normalized to the maximum of the monomer band, one can easily conclude the concentration dependence of the fluorescence spectra of the formed aggregates.

We also investigated the aggregation behavior of 9-vinylanthracene in a PDEGBAC matrix. Figure 3 presents the fluorescence and SFS spectra of the PDEGBAC-9-vinylanthracene polymer system (solid solution, 0.1%). As evident from Figure 2, the spectral aggregation pattern of 9-vinylanthracene in the PDEGBAC matrix exhibits both similarities and distinctions with the solid solutions of anthracene in PMMA (Fig. 2). Since 9-vinylanthracene is predominantly in the form of a solid solution in the polymer, it is evident that a small portion of it copolymerized, as indicated by the weak bands in the fluorescence and SFS spectra at ~λ = 380 nm (Fig. 3).

The aggregates in the SFS spectra (Fig. 3, curve 4) are represented by a weak long-wavelength band. Upon excitation at the maximum of this band, a broad band of excimer-like fluorescence appears, similar to the long-wavelength fluorescence band observed in solid solutions of anthracene in PMMA.

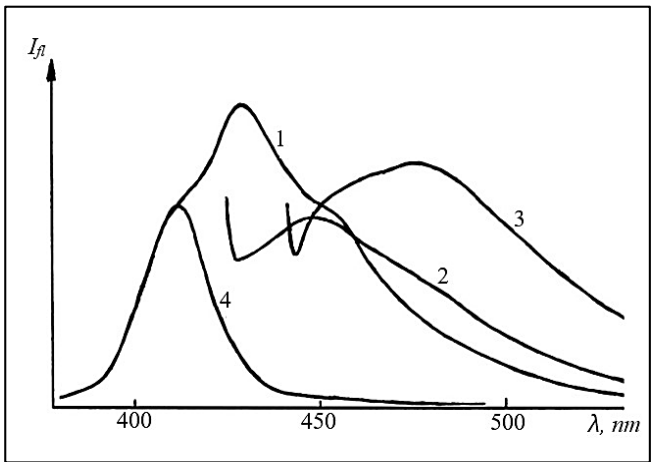

Fig 3: Fluorescence spectra of polymer composites PDEGBAK-9-vinylanthracene recorded at excitation wavelength λ_{exc} = 360(1), 420(2) and 440(3) nm and SFS at $\lambda_{reg} = \lambda_{exc}$+10 nm (4) Wavelengths are indicated according to the registration scale.

9,10-Dibenzanthracene is generally a chromophore that is not prone to aggregation. The benzene substituents at the 9,10-positions of anthracene moiety extend out of the plane of the anthracene core, which creates steric hindrances preventing the overlap of the chromophores' π-systems. However, it can be assumed that within a polymeric matrix, in PVA films, the chromophore adopts a more planar conformation. This planarity likely facilitates aggregate formation, and typical bands of aggregates are observed in the spectra of the copolymer of this structure (Fig. 4).

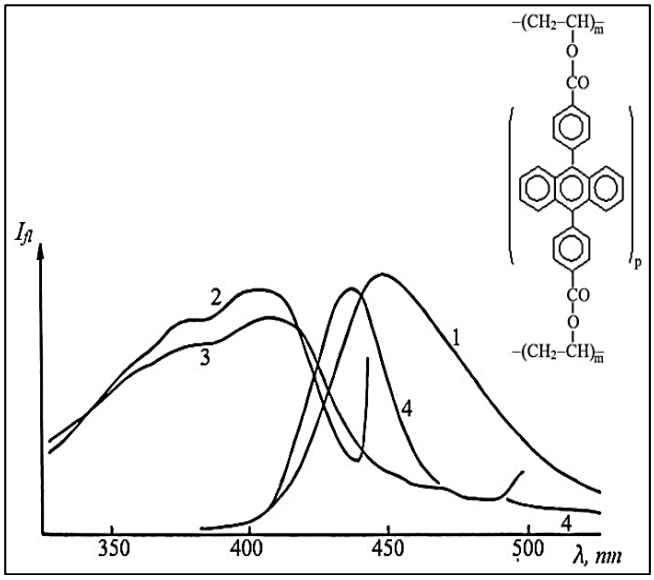

Fig 4: Fluorescence spectra of a PVA copolymer film with a 9,10-dibenzanthracene derivative at excitation wavelength λ_{exc} = 360(1), 450(2) and 520(3) nm and SFS at $\lambda_{reg}=\lambda_{exc}$ + 20 nm (4). Wavelengths are indicated according to the recording scale.

The fluorescence excitation spectrum (λ_{exc} = 450 nm) in the long-wavelength region is slightly broadened and exhibits a bathochromic shift (curve 2) relative to the monomer excitation spectrum (curve 3). In the SFS spectra, several weak components appear in the long-wavelength region (curve 4), which are associated with the formation of aggregates (Fig. 4).

Among the numerous aromatic chromophores prone to aggregate formation, pyrene is the most typical representative. The spectral manifestations of its aggregation in various systems have been investigated in detail by Bains *et al.*, (2021) [35], Yuzhakov (2007) [36], Duhamel (2012) [37]. It is known the pyrene monomer emission is characterized by a combination of five main vibronic bands caused by $\pi \rightarrow \pi^*$ transitions. In addition to the monomer peaks in the range from 425 to 550 nm, centered on ~ 460 nm, a broad unstructured band appears, associated with excimer-type emission (Piñeiro *et al.*, 2015) [38].

Since pyrene excimer emission is highly sensitive to the surrounding environment, several approaches have been developed to spatially restrict excimer formation. These restrictions can affect both the efficiency of excimer formation and the kinetics of their relaxation. One such approach involves precise control of the intermolecular distances between pre-associated pyrene molecules, which can enhance emission intensity. The first studies in this area appeared in 2003. Notably, Thomas *et al.* (2003) [39] employed mesoporous silica to investigate the impact of spatial confinement on pyrene excimer formation.

To illustrate the spectral manifestations of pyrene aggregation, we used two examples in this study: the spectra of pyrene in liquid solutions of chloroform and water.

Figure 5 presents the fluorescence and synchronous fluorescence spectra of a saturated pyrene solution in chloroform (Fig. 5a) and a 1000-fold diluted solution (Fig. 5b), recorded with wavelength offset between the excitation and emission monochromators of $\Delta\lambda$ = 30 nm.

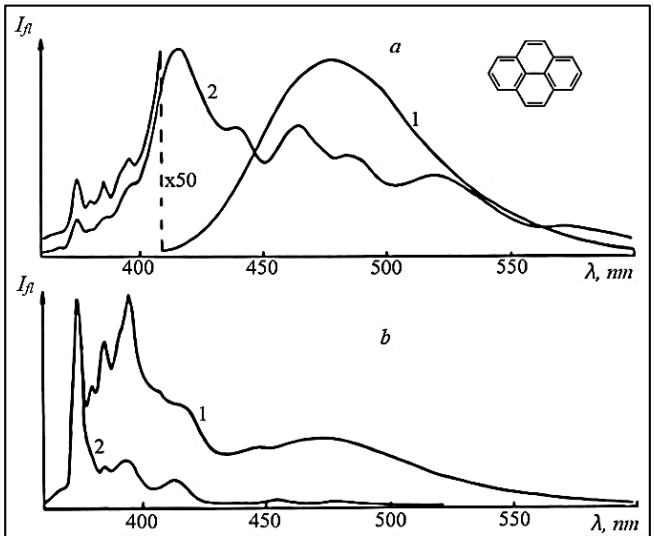

Fig 5: Fluorescence spectra of pyrene solutions in chloroform: saturated (a) and 1000-fold diluted (b) at excitation wavelength λ_{exc}=337 nm (1) and SFS at $\lambda_{reg} = \lambda_{exc}$+30 nm (2). Wavelengths are indicated according to the registration scale.

The concentration dependence of the spectra is revealed not only by comparing the intensities of the excimer and monomer emission bands in conventional fluorescence spectra (Fig. 5 and 6, curve 1), but also by analyzing the positions of the monomer and aggregate bands in the synchronous fluorescence spectra (SFS). In the SFS, a pronounced aggregate band appears in the ~400 nm region, while the narrow, intense band at 375-390 nm corresponds to the pyrene monomer. Additionally, the SFS display a series of low-intensity bands in the 440-480 nm range, corresponding to the excimer fluorescence.

Similar fluorescence and SFS spectra of aqueous pyrene solutions are presented in Figure 6. An intensity band of aggregates is clearly observed in the ~400-410 nm region, while weak excimer fluorescence bands appear in the 430-480

nm range. The SFS spectra were obtained using the same value of $\lambda_{reg} = \lambda_{ex}$ + 30 nm for both solvents, indicating that the solvent nature does not affect the band shapes, nor the separation between the excitation and emission maxima under our experimental conditions. However, Sunuwar *et al.* (2024) [40] reported a strong influence of certain solvents on the position of bands in the SFS spectra of pyrene. The separation between the excitation and emission maxima (Δλ) was 40 nm, 50 nm, and 60 nm in water, *n*-hexane, and ethanol, respectively.

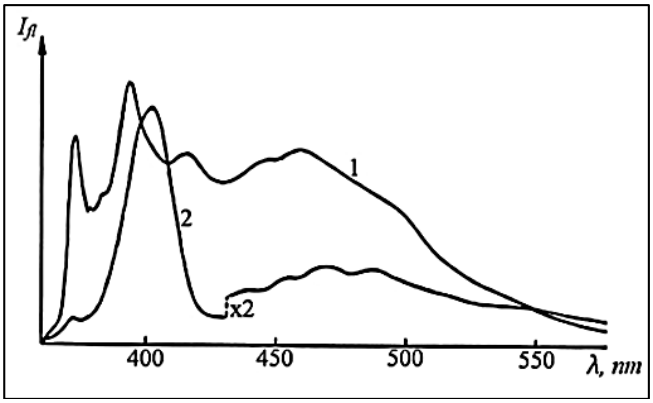

Fig 6: Fluorescence spectra of a saturated pyrene solution in water at excitation λ_{exc}=337 nm (1) and SFS in the registration mode $\lambda_{reg} = \lambda_{exc}$+30 nm (2). Wavelengths are indicated according to the registration scale.

The spectral pattern of aggregation of a naphthalene solid solution in an epoxy polymer matrix (epoxy resin UP-612) (Fig. 7), as copolymers of naphthyl methacrylate with methyl methacrylate (Fig. 8), is rather complex. The monomer fluorescence of naphthalene in the solid solution (λ_{max} ~340 nm) is similar to that observed in liquid solutions of naphthalene, which have been extensively studied Rasouli *et al.* (2016) [41], Zeng *et al.* (2023) [42]. The maximum of the excimer band of naphthalene in solution is at λ_{max} = 390 nm. In the conventional fluorescence spectrum of the solid solution (Fig. 7, curve 1), the excimer band does not exhibit a distinct maximum. However, in the SFS spectrum, within the excimer fluorescence range (370-470 nm), a series bands of aggregates is observed (Fig. 7, curve 2).

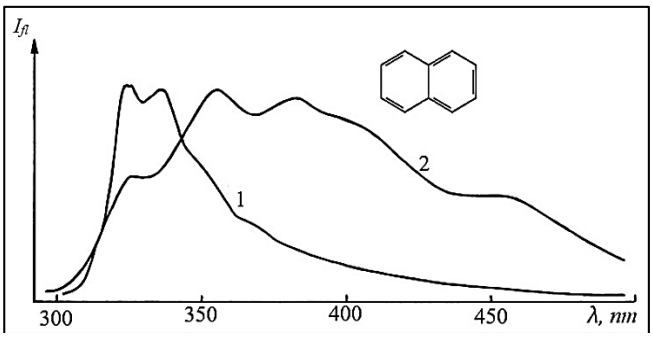

Fig 7: Fluorescence spectra of the composition epoxy resin + 20% naphthalene under excitation at λ_{exc} = 260 nm (1), and SFS at $\lambda_{reg}=\lambda_{exc}$+ 10 nm (2). Wavelengths are given according to the detection scale.

Figure 8 shows the fluorescence spectra of MMA copolymers with naphthyl methacrylate. As can be seen, the monomer fluorescence of the naphthyl fragments in the MMA-naphthyl methacrylate copolymer is represented by a broad band at ~330 nm.

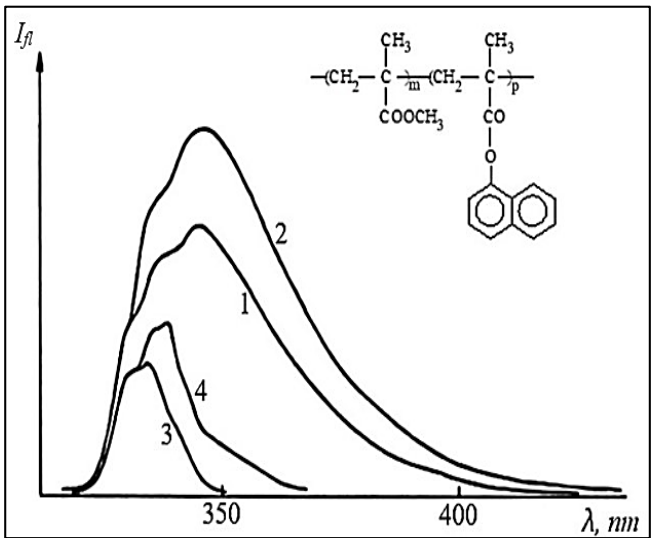

Fig 8: Fluorescence spectra with excitation λ_{exc} =280 nm (1, 2) and SFS (3, 4) of MMA copolymers with naphthyl methacrylate: 0.1 mol% (1, 3) and 0.5 mol% (2, 4). Wavelengths are indicated according to the registration scale.

By comparing spectra 1 and 2 in Figure 8 of the MMA copolymers with naphthyl methacrylate with a different chromophore concentrations, the position of the excimer fluorescence band can be determined, which has a maximum at λ_{max} = 350 nm. The SFS spectra of these samples (0.1 and 0.5 mol%) demonstrate a concentration dependence, also for the aggregate bands (curves 3 and 4).

The most accessible system for studying the aggregation of phenyl chromophores is benzene. However, the high optical density in the benzene monomer fluorescence band creates some difficulties for fluorescence spectra registration. Moreover, the registration of SFS spectra is not possible due to the intense background from the scattered light of the excitation source. Therefore, we registered the fluorescence spectra of benzene at a right angle to the light transmission in a 1 cm cuvette. The obtained spectra are shown in Figure 9.

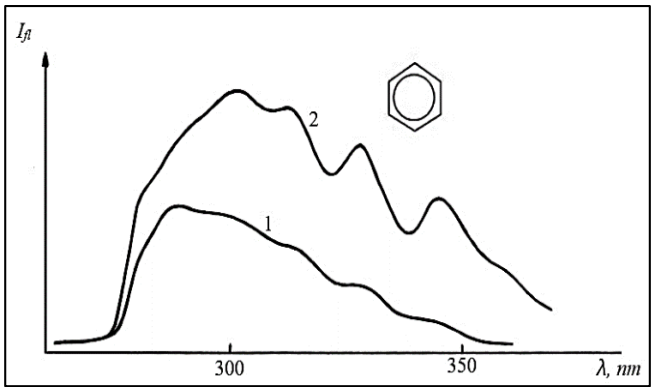

Fig 9: Fluorescence spectra of benzene with λ_{exc} = 254 nm (1) and SFS in the registration mode $\lambda_{reg} = \lambda_{exc}$ + 10 nm (2). Wavelengths are indicated according to the registration scale.

It can be assumed that the spectra are significantly reabsorbed. The monomer fluorescence band of benzene is completely absent, while the excimer fluorescence is represented by a slightly structured band with maxima at λ_{max} = 312, 328, 344 nm (Figure 9, curve 1). The cause of this is likely the formation of aggregates, which are more clearly detected in the SFS spectra (Figure 9, curve 2).

The fluorescence spectra and SFS spectra of benzene can be compared with the spectra of polystyrene film, shown in Figure 10.

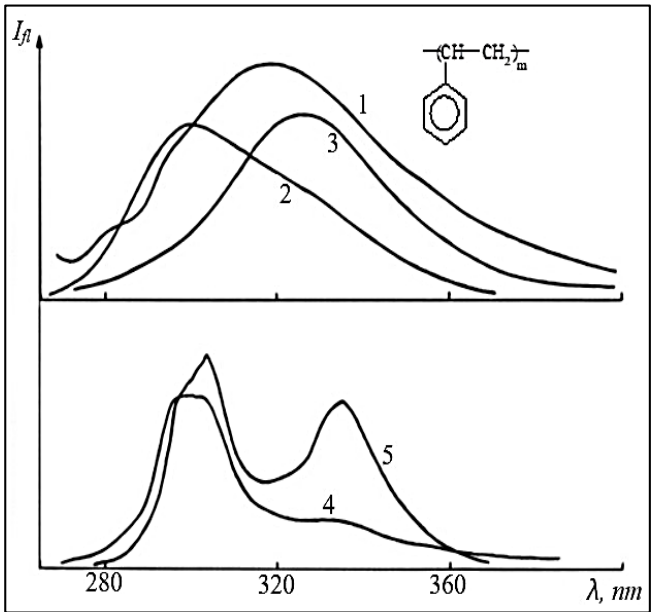

Fig 10: Fluorescence spectra of polystyrene film with excitation λ_{exc} = 254 nm (1) and SFS in the registration modes $\lambda_{reg}=\lambda_{exc}$ (2, 3) and $\lambda_{reg}=\lambda_{exc}+10$ nm (4, 5). Wavelengths are indicated according to the registration scale.

Spectra 3 and 5 were obtained using polarizers. This method involves registering spectra with polarizers oriented perpendicularly, which are placed on the excitation and detection monochromators. Generally, this approach is used for recording SFS spectra of objects that are characterized by significant light scattering. However, in this case, the application of such a method is due to the significant structural differences of the aggregates, which cannot be identified by other methods.

The fluorescence spectrum of a polystyrene sample (Fig. 10, curve 1) contains weakly distinguishable bands of the monomer and excimer, although its appearance is typical for the emission of polymers of this type. At the same time, the SFS spectra of polystyrene sample (Fig. 10, curves 2-5) demonstrate the formation of several types of aggregates of chromophore fragments. Differentiation of the aggregates becomes possible when comparing SFS spectra obtained in different scanning modes (curve 2 and 3, curve 4 and 5), and with the use of polarizers (curve 3 and 5).

Generalization on Component Identification in SFS Spectra

Based on spectral studies of a model series of polymer systems containing different chromophores, it is possible to generalize the approach to component identification in SFS spectra. The analysis shows that all SFS spectra of the studied systems contain aggregate bands of the chromophores, which are bathochromically shifted relative to the corresponding monomer bands. The confirmation of this regularity is the fact that the spectral features of aggregation are common both for different chromophores and for different systems (Yuzhakov, 1992) [15]. Thus, it can be stated that the aggregates of aromatic chromophores have to vary degrees bathochromically shifted 0-0 transition bands and their fluorescence is predominantly excimer-like.

Obviously, the emergence of excimer-like fluorescence is due to the formation of aggregates with different structures, which contain varying numbers of chromophore moiety, depending on the nature of the studied object. In the case of copolymers or homopolymers like polystyrene, the simplest form of an aggregate is a dimer, consisting of two molecular subunits connected through non-covalent π-π interactions. The probability of forming more complex structures, consisting of three or more closely positioned chromophore groups, is minimal due to steric hindrances (Pompetti *et al.*, 2024) [43]. In liquid solutions, especially in saturated ones, as well as in solid solutions of chromophores in polymers, aggregates can be complexes with numerous molecules or even microcrystals. In solutions of tetracene in THF and dimethylformamide, the formation of dimers connected by covalent bridges – allowing for variation in chromophore distance and relative orientation – was reported by Miller *et al.* (2023) [44].

Tetracene films and crystals have a well-defined and rigid intermolecular geometry, governed by electrostatic or van der Waals forces, and chromophore aggregation occurs in the form of different microcrystalline formations, which vary in fluorescence color (Yan *et al.*, 2020) [45].

The predominant form of pyrene aggregates is the dimer. Pyrene dimers, formed via covalent or supramolecular interactions, readily generate "static excimers" which typically result in enhanced emission. Such emission enhancement can be achieved through precise control of intermolecular distances between pre-associated molecules. Since pyrene excimer emission is highly sensitive to the local environment, spatial confinement (via encapsulation or incorporation into a polymer matrix) can enhance excimer fluorescence, as demonstrated by Piñeiro *et al.* (2015) [38], Thomas *et al.* (2003) [39].

Thus, the excimer-like fluorescence of various aggregates represents the fluorescence of dimers capable of relaxing into an excimer geometry (Hoche *et al.*, 2017) [22].

It should be noted that the components in the SFS spectra obtained under different registration modes, especially in the $\lambda_{reg} = \lambda_{exc}$, cannot reflect the population of energy levels of different aggregate states, since after excitation the aggregates are capable of relaxing into the most stable structure for them. The SFS spectra of pyrene solutions in water and chloroform are particularly illustrative in this regard (Fig. 5, 6). In both solvents, the SFS spectra exhibit an intense band of aggregates with a maximum at 400 nm. In the region of the excimer fluorescence maximum, these spectra also show a series of relatively intense bands.

The systems considered in this study, in addition to common features of the spectral manifestations of chromophore aggregation, also exhibit individual characteristics. In the synchronous fluorescence spectra (SFS) of solid solutions of anthracene in PMMA (0.5-2%), a single dominant spectral maximum at 400 nm is observed (Fig. 2, curves 3 and 4), which may suggest the formation of single type aggregates. The conventional fluorescence spectra show no bands with a pronounced Stokes shift; only in the more bathochromic region (Fig. 2, curve 2) does a broad band of the excimer-like fluorescence appear, presumably due to aggregates of a different structure. This indicates that these aggregates in the excited state do not relax to the excimer geometry and are, in fact, T-type dimers. As is known, anthracene dimers can have four possible structures: normal dimer, twisted dimer, offset dimer and T-shaped dimer (Zhao *et al.*, 2018) [46].

However, based on the band position of the 0-0 transition, it can be assumed that the dimers in solid solutions of anthracene in PMMA adopt a "sandwich" structure in the ground state, which promotes excimer formation and leads to the appearance of a broad fluorescence band with a significant Stokes shift.

The spectral pattern of aggregation for 9-vinylanthracene in PDEGBAC (Fig. 3) and for the PVA copolymer with 9,10-dibenzanthracene (Fig. 4) differs from that observed in solid solutions of anthracene in PMMA by the absence of well-defined aggregate bands. In the SFS spectra of these systems, the formation of aggregates leads to the appearance of a long-wavelength tail band, and excitation into this band results in excimer-like fluorescence occurs. This difference is likely due to the presence of substituents on the anthracene core, which introduce steric hindrance and prevent the formation of T-type aggregates.

The studied chromophores' – anthracene, 9-vinylanthracene, 9,10-dibenzanthracene-have the lowest excited singlet S1 state of ^1L_a nature. The high intensity of $S_0 \rightarrow S_1$ transitions in the monomers makes the monomeric component dominant in the SFS spectra. In pyrene, naphthalene and benzene molecules, the lowest singlet excited state (S_1) has the character ^1L_b, which explains the significantly lower intensity of the transitions bands. This likely explains the predominance of aggregate spectral bands in the SFS spectra of systems containing these chromophores, especially at sufficiently high concentrations (Figs. 5-7, 9, 10).

The spectral features of chromophore aggregation in MMA copolymers with naphthylmethacrylate differ somewhat from the systems discussed above (Fig. 8). In the SFS spectra, the aggregate components exhibit a slight bathochromic shift relative to the monomer band, and their intensity is comparable to that of the monomer.

Conclusions

Conventional fluorescence spectroscopy has certain limitations when analyzing multicomponent systems due to the spectral overlap of excitation and emission bands. Synchronous fluorescence spectroscopy (SFS), by simultaneously scanning excitation and emission wavelengths with a constant wavelength interval ($\Delta\lambda$), significantly improves spectral resolution and allows for better discrimination of individual components within complex systems. This method provides enhanced spectral resolution, suppresses scattering interference, highlights subtle spectral features, and improves selectivity in detecting specific fluorescent species. In this study, the capabilities of SFS were demonstrated for the differentiation of monomeric and excimeric emission bands in various systems, including both solution and solid-state polymer matrices. The results clearly show that SFS enables precise identification of aggregate-related spectral features, such as bathochromic shifts and excimer-like emission that are often masked in conventional fluorescence spectra. Overall, SFS proves to be a highly effective and sensitive spectroscopic tool for probing aggregation phenomena in chromophore-containing polymer systems and can significantly contribute to the rational design of luminescent materials with tailored photophysical properties.

Conflicts of Interest

The authors indicated that there were no potential conflicts of interest to declare.

Funding

No funding for this work.

References

1. Weldeab AO, Li L, Cekli S, Abboud KA, Schanze KS, Castellano RK. Pyridine-terminated low gap π-conjugated oligomers: Design, synthesis, and photophysical response to protonation and metalation. Org Chem Front. 2018;5:3170-3177. DOI: https://doi.org/10.1039/C8QO00963E
2. Saremi B, Bandi V, Kazemi S, Hong Y, D'Souza F, Yuan B. Exploring NIR Aza-BODIPY-based polarity sensitive probes with ON-and-OFF fluorescence switching in Pluronic nanoparticles. Polymers (Basel). 2020;12:540. DOI: https://doi.org/10.3390/polym12030540
3. Yamagishi H, Matsui T, Kitayama Y, Aikyo Y, Tong L, Kuwabara J, *et al*. Fluorescence switchable conjugated polymer microdisk arrays by cosolvent vapor annealing. Polymers (Basel). 2021;13:269. DOI: https://doi.org/10.3390/polym13020269
4. Li Q, Zhang W-C, Wang C-F, Chen S. In situ access to fluorescent dual-component polymers towards optoelectronic devices via inhomogeneous biphase frontal polymerization. RSC Adv. 2015;5:102294-102299. DOI: https://doi.org/10.1039/C5RA19173D
5. Liu Y, Wang Y-M, Zhu W-Y, Zhang C-H, Tang H, Jiang J-H. Conjugated polymer nanoparticles-based fluorescent biosensor for ultrasensitive detection of hydroquinone. Anal Chim Acta. 2018;1012:60-65. DOI: https://doi.org/10.1016/j.aca.2018.01.027
6. Lichon L, Kotras C, Myrzakhmetov B, Arnoux P, Daurat M, Nguyen C, *et al*. Polythiophenes with cationic phosphonium groups as vectors for imaging, siRNA delivery, and photodynamic therapy. Nanomaterials. 2020;10:1432. DOI: https://doi.org/10.3390/nano10081432
7. Korneev OV, Sakhno TV, Korotkova IV. Nanoparticles-based photosensitizers with effect of aggregation-induced emission. Biopolym Cell. 2019;35(4):249-267. DOI: http://dx.doi.org/10.7124/bc.000A08
8. Li C, Xu Y, Liu Y, Ren Z, Ma Y, Yan S. Highly efficient white-emitting thermally activated delayed fluorescence polymers: Synthesis, non-doped white OLEDs and electroluminescent mechanism. Nano Energy. 2019;65:104057. DOI: https://doi.org/10.1016/j.nanoen.2019.104057
9. Jiang N, Zhu D, Su Z, Bryce MR. Recent advances in oligomers/polymers with unconventional chromophores. Mater Chem Front. 2021;5:60-75. DOI: https://doi.org/10.1039/d0qm00626b
10. Bu Q, Li P, Xia Y, Hu D, Li W, Shi D, *et al*. Design, synthesis, and biomedical application of multifunctional fluorescent polymer nanomaterials. Molecules. 2023;28(9):3819. DOI: https://doi.org/10.3390/molecules28093819
11. De Acha N, Elosua C, Matias I, Arregui FJ. Luminescence-based optical sensors fabricated by means of the layer-by-layer nano-assembly technique. Sensors (Basel). 2017;17(12):2826. DOI: https://doi.org/10.3390/s17122826
12. Huang Y, Xing J, Gong Q, Chen LC, Liu G, Yao C, *et al*. Reducing aggregation caused quenching effect through co-assembly of PAH chromophores and molecular barriers. Nat Commun. 2019;10(1):169. DOI: https://doi.org/10.1038/s41467-018-08092-y

13. Ahumada G, Borkowska M. Fluorescent polymers conspectus. Polymers (Basel). 2022;14(6):1118. DOI: https://doi.org/10.3390/polym14061118
14. Fakis M, Anestopoulos D, Giannetas V, Persephonis P. Influence of aggregates and solvent aromaticity on the emission of conjugated polymers. J Phys Chem B. 2006;110(49):24897-24902. DOI: https://doi.org/10.1021/jp0619033
15. Yuzhakov VI. Aggregation of dye molecules and its influence on the spectral luminescent properties of solutions. Russ Chem Rev. 1992;61(6):613-628. DOI: https://doi.org/10.1070/RC1992v061n06ABEH000988
16. Ma S, Du S, Pan G, Dai S, Xu B, Tian W. Aggregate. 2021;2:e96. DOI: https://doi.org/10.1002/agt2.96
17. Heo J, Murale DP, Yoon HY, Arun V, Choi S, Kim E, *et al*. Recent trends in molecular aggregates: An exploration of biomedicine. Aggregate. 2022;3:e159. DOI: https://doi.org/10.1002/agt2.159
18. Schillmöller T, Herbst-Irmer R, Stalke D. Insights into excimer formation factors from detailed structural and photophysical studies in the solid-state. Adv Optical Mater. 2021;9:2001814. DOI: https://doi.org/10.1002/adom.202001814
19. Gao Y, Liu H, Zhang S, Gu Q, Shen Y, Ge Y, *et al*. Excimer formation and evolution of excited state properties in discrete dimeric stacking of an anthracene derivative: A computational investigation. Phys Chem Chem Phys. 2018;20:12129-12137.
20. Zhao Y, Xu P, Zhang K, Schönherr H, Song B. Strong emission of excimers realized by dense packing of pyrenes in tailored bola-amphiphile nano assemblies. Cell Rep Phys Sci. 2022;3(2):100734. DOI: https://doi.org/10.1016/j.xcrp.2021.100734
21. Lee J, Jung H, Shin H, Kim J, Yokoyama D, Nishimura H, *et al*. Excimer emission based on control of molecular structure and intermolecular interactions. J Mater Chem C. 2016;4(14):2784-2792. DOI: https://doi.org/10.1039/C5TC03289J
22. Hoche J, Schmitt HC, Humeniuk A, Fischer I, Mitric R, Rohr MIS. The mechanism of excimer formation: An experimental and theoretical study on the pyrene dimer. Phys Chem Chem Phys. 2017;19:25002-25015.
23. Li W, Wang L, Zhang J, Wang H. Bis-pyrene-based supramolecular aggregates with reversibly mechanochromic and vapochromic responsiveness. J Mater Chem C. 2014;2:1887-1892.
24. Chen Y. Recent advances in excimer-based fluorescence probes for biological applications. Molecules. 2022;27(23):8628. DOI: https://doi.org/10.3390/molecules27238628
25. Dai Y, Rambaldi F, Negri F. Eclipsed and twisted excimers of pyrene and 2-azapyrene: How nitrogen substitution impacts excimer emission. Molecules. 2024;29(2):507. DOI: https://doi.org/10.3390/molecules29020507
26. Casier R, Duhamel J. Pyrene Excimer Formation (PEF) and Its Application to the Study of Polypeptide Dynamics. Langmuir. 2022;38(12):3623-3629. DOI: https://doi.org/10.1021/acs.langmuir.2c00129
27. Lloyd JBF. Synchronized excitation of fluorescence emission spectra. Nat Phys Sci. (Lond.). 1971;231:64-65. DOI: https://doi.org/10.1038/physci231064a0
28. Vo-Dinh T. Multicomponent analysis by synchronous luminescence spectrometry. Anal Chem. 1978;50:396-401. DOI: https://doi.org/10.1021/ac50025a010
29. Cabaniss SE. Theory of variable-angle synchronous fluorescence spectra. Anal Chem. 1991;63:1323-1327. DOI: https://doi.org/10.1021/ac00013a027
30. Tian M, Muhammad T, Li Y, Fan X, Wang L, Mi F. Application of synchronous fluorescence spectroscopy in the analysis of polycyclic aromatic hydrocarbons in petroleum and coal. Appl Spectrosc Rev. 2025;1-27. DOI: https://doi.org/10.1080/05704928.2025.2476420
31. Samokhvalov A. Analysis of various solid samples by synchronous fluorescence spectroscopy and related methods: A review. Talanta. 2020;216:120944. DOI: https://doi.org/10.1016/j.talanta.2020.120944
32. Silveira AL, Barbeira PJS. Synchronous fluorescence spectroscopy and multivariate classification for the discrimination of cachaças and rums. Spectrochim Acta A Mol Biomol Spectrosc. 2022;270:120821. DOI: https://doi.org/10.1016/j.saa.2021.120821
33. Luo WA, Cheng L, Dai LZ, Chen XD, Mai KC, Chen YJ, *et al*. Polymer crystallization dynamics investigated by synchronous scanning spectrum. Guang Pu Xue Yu Guang Pu Fen Xi. 2014;34(9):2320-2326. PMID: 25532318
34. Congrave DG, Drummond BH, Gray V, Bond AD, Rao A, Friend RH, *et al*. Suppressing aggregation induced quenching in anthracene based conjugated polymers. Polym Chem. 2021;12:1830-1836. DOI: https://doi.org/10.1039/d1py00118c
35. Bains GK, Kim SH, Sorin EJ, Narayanaswami V. The extent of pyrene excimer fluorescence emission is a reflector of distance and flexibility: analysis of the segment linking the LDL receptor-binding and tetramerization domains of apolipoprotein E3. Biochemistry. 2012;51(31):6207-6219. DOI: https://doi.org/10.1021/bi3005285
36. Yuzhakov VI. Aggregation of dye molecules and its influence on the spectral luminescent properties of solutions. Russ Chem Rev. 2007;61(6):613-628. DOI: https://doi.org/10.1070/RC1992v061n06ABEH000988
37. Duhamel J. New Insights in the Study of Pyrene Excimer Fluorescence to Characterize Macromolecules and their Supramolecular Assemblies in Solution. Langmuir. 2012;28(16):6527-6538.
38. Piñeiro L, Novo M, Al-Soufi W. Fluorescence emission of pyrene in surfactant solutions. Adv Colloid Interface Sci. 2015;215:1-12. DOI: https://doi.org/10.1016/j.cis.2014.10.010
39. Thomas A, Polarz A, Antonietti M. Influence of spatial restrictions on equilibrium reactions: A case study about the excimer formation of pyrene. J Phys Chem B. 2003;107:5081-5087.
40. Sunuwar S, Haddad A, Acheson A, Manzanares CE. Synchronous Fluorescence as a Sensor of Trace Amounts of Polycyclic Aromatic Hydrocarbons. Sensors. 2024;24(8):3800.
41. Rasouli M, Tavassoli SH, Mousavi SJ, Darbani SMR. Measuring of naphthalene fluorescence emission in the water with nanosecond time delay laser induced fluorescence spectroscopy method. Optik. 2016;127(15):6218-6223. DOI: https://doi.org/10.1016/j.ijleo.2016.04.081
42. Zeng C, Xu Z, Song C, Qin T, Jia T, Zhao C, *et al*. Naphthalene-based fluorescent probe for on-site detection of hydrazine in the environment. J Hazard Mater. 2023;445:130415. DOI: https://doi.org/10.1016/j.jhazmat.2022.130415

43. Pompetti NF, Smyser KR, Feingold B, Owens R, Lama B, Sharma S, *et al*. Tetracene Diacid Aggregates for Directing Energy Flow toward Triplet Pairs. J Am Chem Soc. 2024;146(16):11473-11485.
DOI: https://doi.org/10.1021/jacs.4c02058
44. Miller EG, Singh M, Parkin S, Sammakia T, Damrauer NH. Preparation of a Rigid and Nearly Coplanar Bis-Tetracene Dimer through an Application of the CANAL Reaction. J Org Chem. 2023;88(17):12251-12256. DOI: https://doi.org/10.1021/acs.joc.3c00809
45. Yan X, Liu H, Wang X, Liu S, Zhao D, Tang Z, *et al*. Singlet Fission in Self-Assembled Amphipathic Tetracene Nanoparticles: Probing the Role of Charge-Transfer State. J Photochem Photobiol A Chem. 2020;397:112597.
DOI: https://doi.org/10.1016/j.jphotochem.2020.112597
46. Zhao C, Cai X, Ma Z, Shi J, Xu L, Wang H. Excimer formation from partially overlapped anthracene dimer based on saddle-shaped cyclooctatetrathiophene as spacer. J Photochem Photobiol A Chem. 2018;355:318-325.
DOI: https://doi.org/10.1016/j.jphotochem.2017.08.030